Heat-Transfer Characteristics in Viscous Gas-Liquid and Gas-Liquid-Solid Systems

Samir Kumar and L.-S. Fan
Dept. of Chemical Engineering, The Ohio State University, Columbus, OH 43210

Local heat-transfer measurements are performed using a special heat-transfer probe in gas-liquid and gas-liquid-solid systems with viscous Newtonian liquids as the continuous phase. Effects of viscosity on bubble-liquid and bubble-liquid-solid interactions affecting local heat transfer are studied through heat-transfer experiments with simultaneous flow visualization in a simplified system involving single bubbles or a chain of gas bubbles moving in viscous liquids and liquid-solid systems. Effects of viscosity on bubble wake and local heat transfer are examined with reference to heat transfer in freely-bubbling beds (bubble columns and three-phase fluidized beds). The kinematic viscosity of the fluid greatly influences the nature of flow in the wake which affects local heat transfer in the bed. The local heat transfer decreases with the viscosity due to the rapid decay in the circulation strength of the bubble wake caused by increased viscous dissipation of vorticity. Local heat transfer due to cyclic/periodic injection of bubbles is significantly enhanced due to increased bubble-wake interactions which rapidly accelerate bubbles and increase average bubble rise velocity. Heat transfer in simplified liquid and liquid-solid systems with single- and chain-bubble injections characterizes the local heat-transfer performance of freely-bubbling beds (bubble columns and three-phase fluidized beds). A mechanistic model developed accounts for the heat-transfer behavior in bubble columns and three-phase fluidized beds with viscous liquids.

Introduction

Three-phase fluidized-bed reactors have been widely used in hydrogenation, oxidation, polymerization reactions, and biotechnological and petroleum processes (Deckwer, 1985; Fan, 1989). Previous reviews (Epstein, 1981; and Fan, 1989) noted that most of the experimental work in gas-liquid-solid fluidized beds deal with low-viscosity Newtonian liquids as the continuous phase. In particular, major emphases were on hydrodynamics, which include phase holdups, bubble sizes and their distribution, axial and radial dispersion of liquids, wake sizes and wake solids holdups, as well as mass- and heat-transfer studies. In contrast, relatively few studies have been performed concerning the hydrodynamics, mass and heat transfer in three-phase fluidized beds with viscous Newtonian or non-Newtonian liquids as the continuous phase (Kato et al., 1981; Kang et al., 1985; Patwari et al., 1986; Zaidi et al., 1990; Grandjean et al., 1990). Due to increasing applications of three-phase fluidized beds with viscous Newtonian and/or non-Newtonian liquids in fermentation, polymer production, and food processing, a fundamental understanding of transport phenomena in these systems is of considerable importance.

Heat-transfer studies in three-phase fluidized beds have been concerned mainly with the measurements of time-averaged heat transfer in a low/moderate-viscosity Newtonian liquid. A comprehensive review is given by Kim and Laurent (1991). While much progress has been made in understanding heat transfer in low/moderate-viscosity systems, information on the heat-transfer behavior in bubble columns and three-phase fluidized beds with viscous Newtonian/non-Newtonian liquids as the continuous phase is rather sparse. Kim and Laurent (1991) reported that the heat-transfer coefficient decreases with viscosity, independent of the particle size and fluid velocities. Kang et al. (1985) attributed this decrease to the increase of the thickness of the laminar viscous sublayer around the heater

Correspondence concerning this article should be addressed to S. Kumar at Xerox Corporation, 800 Phillips Road O143-02S, Webster, NY 14580.

surface, decrease of turbulence, and increase of viscous friction losses between phases. Furthermore, within the range of their study (μ_l= 1-39 cp), they speculated that this decrease may be caused by the increase in bubble size and rise velocity due to enhanced bubble coalescence with the increase of liquid viscosity which results in decreasing gas holdup and, thereby, heat transfer. However, this explanation is highly suspect as the increased bubble size and rise velocity are reported to increase the local heat transfer (Kumar et al., 1992). Bubble motion and the associated wake flows are believed to be responsible for the above-mentioned transport phenomena in multiphase systems (Fan and Tsuchiya, 1990). Recently, Kumar et al. (1992) provided a mechanistic understanding of the heat transfer in bubbly liquid and liquid-solid systems with low-viscosity Newtonian liquid (water) as the continuous phase. They reported that the heat-transfer enhancement due to the passage of a single gas bubble is caused by the bubble wake which is primarily responsible for the rapid surface renewal of fluid on the heat-transfer surface. Furthermore, the enhancement in heat transfer due to the bubble increases with its size because of the increased surface renewal caused by larger bubble wake and stronger vortices. Therefore, to better understand the extremely complex flow structure in bubble column and three-phase viscous systems and its effects on the pertinent hydrodynamic properties and heat- and mass-transfer characteristics, it is necessary to understand a simplified system involving a single bubble or a chain of bubbles moving in a viscous Newtonian or non-Newtonian liquid and liquid-solid systems.

The purpose of this study is to understand the mechanisms of heat transfer in bubble columns and three-phase fluidized beds with Newtonian liquids of different viscosities. It has been well known that the kinematic viscosity of the liquid has a great influence on the nature of the flow in the wake which affects the local transport properties such as the heat transfer.

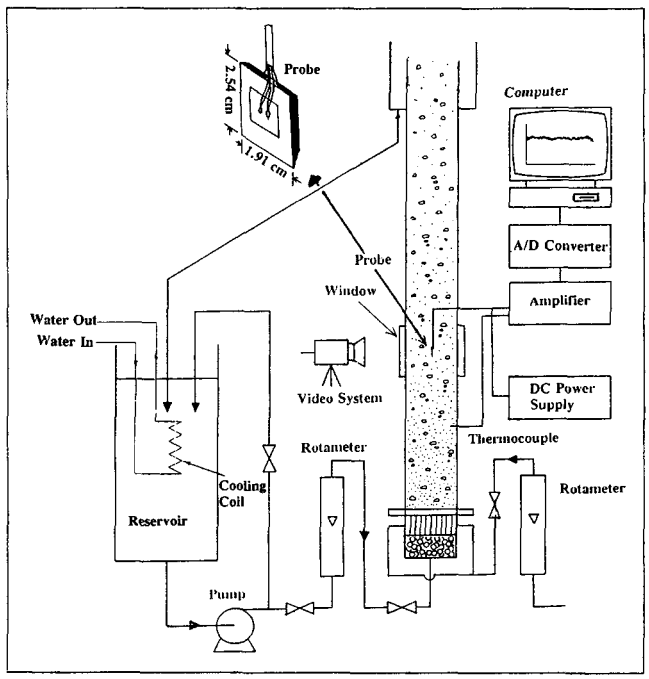

Figure 1. Experimental setup.

Therefore, to understand the viscosity effect on the heat transfer, local instantaneous heat-transfer measurements are performed by introducing a single bubble and/or a chain of gas bubbles in a liquid and liquid-solid fluidized bed with liquids of varying viscosities as the continuous phase. The heat-transfer results obtained in the simplified systems are examined with reference to the heat-transfer characteristics in freely-bubbling beds (bubble columns and three-phase fluidized beds).

Experimental Studies

The experimental apparatus is shown in Figure 1. The experiments are conducted in a three-dimensional Plexiglas column, 150 cm high and 7.62 cm ID. Liquid enters the column through a packed layer of 6-mm glass beads, and a steady liquid velocity is maintained by circulating water through a reservoir and a rotary pump. The bulk temperature is maintained constant during the experimental run by circulating cold water through the cooling coil. The fluid physical properties are evaluated at the bulk temperature. Air is used as the gas phase, while either water (μ_l= 0.86 cp) or aqueous glycerin solutions of different viscosities (μ_l= 38.5-98.5 cp) is the liquid phase. The fluidized particles used are 163-μm (GB163), 760 = μm (GB760), and 1-mm (GB1000) glass beads.

The local instantaneous heat-transfer coefficient h_i is measured by a special heat-transfer probe (Kumar et al., 1992) and is obtained from the instantaneous change in the temperature difference, ΔT_i, and the time-averaged heat-transfer rate, Q:

$$h_i = Q/\Delta T_i \tag{1}$$

where $\Delta T_i = (T_{si} - T_\infty)$. The heat flux sensor directly measures Q and T_{si} while T_∞ is measured by another thermocouple flushed with the column wall. Typical differential temperature ΔT_i in the stagnant liquid medium is 10°C, while that in the bubble column is 4°C.

The local time-averaged heat-transfer coefficient is obtained by averaging the instantaneous heat-transfer coefficient data over a number of sampling points as:

$$h_{av} = \frac{1}{n}\sum_{i=1}^{n}\frac{Q}{\Delta T_i} \tag{2}$$

The probe is located along the column axis with the aid of a support 52 cm above the distributor. Due to the small width (0.32 cm) of the probe at a horizontal section of the column, the disturbance to the flow field in the vicinity of the probe is minimal, and the measured instantaneous heat-transfer rate by the probe is a direct measure of the local instantaneous heat-transfer coefficient in the bed at that particular location. Signals for the heat flux as well as the temperature difference between the probe surface and the bulk are sampled simultaneously at the rate of 180 Hz for 11 s, and the high-frequency noise in the original signal is reduced by smoothing the signals employing a low-pass software filter.

Single spherical-cap bubbles are injected without any pressure perturbation or satellites generation in liquid and liquid-solid systems with high-viscosity liquids by employing a three-dimensional hemispherical cup located 10 cm above the distributor. As shown in Figure 2, a chain of gas bubbles of

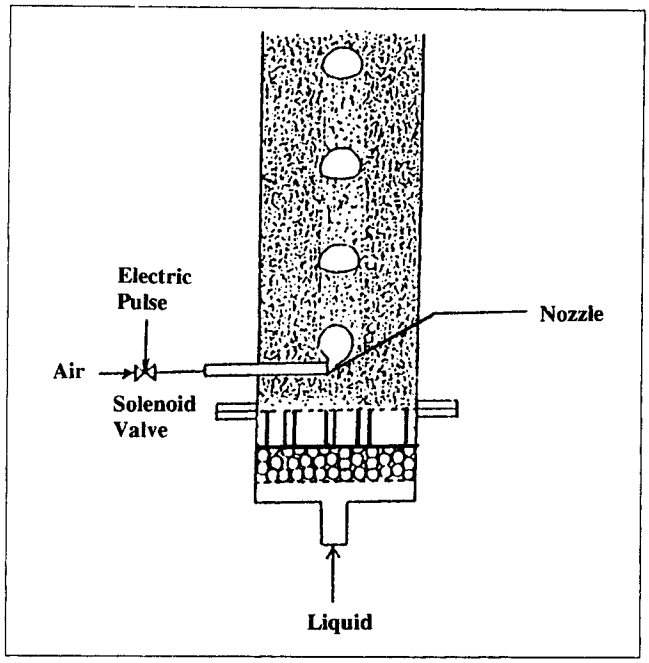

Figure 2. Setup for the formation of a stream of bubbles in liquids and liquid-solid fluidized beds.

initially equal size and spacing are injected from a 4-mm-ID nozzle which is fixed horizontally on the column wall 10 cm above the gas-liquid distributor. The bubble formation frequency (f) is varied from 0.87-2.82 s^{-1} by varying the frequency of electric pulse signal which activates a solenoid valve. The bubble size can be altered by varying the pulse width which controls the opening time of the solenoid valve. At lower pulse widths, a chain of spherical cap bubbles of initially equal size and spacing is introduced in the column, while at larger pulse widths, a chain of slug bubbles (Taylor bubbles) is formed which is typical of a highly viscous continuous phase. During each experimental run, simultaneous visualization is performed with heat-transfer measurements to identify specific effects of bubble wake-liquid and bubble wake-liquid-solid interactions on heat-transfer characteristics in viscous Newtonian systems. Details of the probe design and measurement techniques including flow visualization are given by Kumar et al. (1992).

Modeling

An attempt is made to propose mechanisms for heat-transfer enhancement by chain bubbling/free-bubbling in liquid and liquid-solid systems based on the available models for heat transfer. For a single bubble injection in the low-viscosity liquid ($\mu_l = 0.86$ cp), Kumar et al. (1992) proposed a mechanism based on the consecutive film-penetration theory by Wasan and Ahluwalia (1969) which successfully predicted the local heat-transfer enhancement caused by the bubble. Due to the small dimensions of probe, it may be assumed that all the fluid elements renew the probe surface at the same rate, and there is no distribution of residence time. Kumar et al. (1992) observed that the local maximum in the heat transfer lies in the near wake which resides immediately behind a rising bubble and moves in close association with the bubble. Based on their observation, they concluded that during the increased heat transfer due to each bubble in the heat-transfer signal, the absolute bubble rise velocity can be taken as an estimate of the characteristic velocity of a fluid element near the heat-transfer surface, and the film thickness at the probe surface can be calculated based on the absolute bubble rise velocity. Therefore, during the heat-transfer enhancement by the bubble wake, the time available for heating by conduction before each fluid element passes the heat-transfer surface may be approximated as:

$$t_c = L/U_b \tag{3}$$

and during this time unsteady heat conduction occurs over a distance, δ.

According to the criterion given by Toor and Marchello (1958), the residence time calculated is in the region where unsteady heat absorption controls. Therefore, surface renewal/penetration model and film-penetration model can be applied. The surface renewal/penetration model gives:

$$h'_{av} = 2(\rho_l C_{pl} k/\pi t_c)^{1/2} \tag{4}$$

where $t_c = L/U_b$ and h'_{av} is the average heat-transfer coefficient over t_c. In Eq. 4, the physical properties would be fixed for a given system and only t_c is a variable which depends on the bubble dynamics. Using this model, the value of h'_{av} for the case of a single-bubble injection ($V_b = 5$ cm^3) in the viscous liquid (Figure 3) is 3638.77 $W/m^2 \cdot K$, which is much higher than the experimental value ($h'_{av} = 684.10$ $W/m^2 \cdot K$). Thus, the surface renewal/penetration model over-predicted the local heat-transfer enhancement behind bubbles by an order of magnitude. Tuot and Clift (1973) also reported that the surface renewal/penetration and film-penetration models for unsteady heat transfer in a gas-solid fluidized bed greatly overpredict the transient heat transfer behind each bubble. They, however, reported that Eq. 4 with $t_c = L/U_b$ does explain the relatively slow decrease of h_i after the maximum behind the bubble and concluded that the form of Eq. 4 is valid although the constant value is in error. They speculated that the difference could be ascribed to a gas film at the heater surface in a gas-solid fluidized bed. In an analogous manner, in the present gas-liquid and gas-liquid-solid systems it is believed that a thin liquid film of thickness δ exists at the probe surface and the mass of fluid brought by the bubble wake is viewed to exchange heat by unsteady-state conduction at the outer edge of the film. The resistance to heat transfer is due to the film (whose thickness depends on the liquid properties and the local hydrodynamics) followed by penetration and unsteady-state heating of an element. The presence of a thin liquid film at the probe surface is also substantiated by the fact that the instantaneous heat transfer does not show a sharp drop when the bubble comes in direct contact with the probe (Figure 3). As the Peclet number, Pe ($= Re\ Pr$) is large under the present experimental conditions, very small convection velocities can overwhelm thermal conduction, and heat-transfer process becomes convection-dominated at a very short distance from the probe surface. Thus, before the heat released from the probe can propagate very far in the lateral direction, it is swept into the wake. The fluid elements brought by the bubble wake of each bubble renews the probe surface, and the temperature of the fluid element sweeping the outer surface of the film is assumed

to be uniform and equal to the bulk temperature, T_∞. Thus, essentially the heat-transfer phenomenon is a sequential process of diffusion followed by convection. Based on these assumptions and applying the consecutive film and surface renewal theory, the average of the instantaneous heat-transfer coefficient over the contact time, t_c is given as:

$$h'_{av}=\frac{2k}{\sqrt{(\pi\alpha t_c)}}+\frac{k\delta}{\alpha t_c}\left[e^{\frac{\alpha t_c}{\delta^2}}\left(1-\text{erf}\,\frac{\sqrt{(\alpha t_c)}}{\delta}\right)-1\right] \quad (5)$$

It is interesting to note that as $(\alpha t_c)^{1/2}/\delta\to 0$, $h'_{av}\delta/k\to 1$ and as $(\alpha t_c)^{1/2}/\delta\to\infty$, $h'_{av}=2k/(\pi\alpha t_c)^{1/2}$, that is, under proper limiting conditions, the consecutive film and surface renewal model reduces to the film theory and the penetration theory, respectively.

This model requires a correct estimation of the film thickness. In the present study with viscous liquids, the film thickness δ is estimated based on the border diffusion layer model (Azbel, 1981). According to this model, in the boundary layer, both momentum and heat are transferred by means of turbulent eddies. However, very close to the wall in the viscous sublayer, turbulent eddies become small and the momentum transfer by molecular viscosity exceeds that by turbulent eddies, and the temperature decreases appreciably faster. In the viscous sublayer, more heat is still transferred by turbulent diffusion and only in the immediate vicinity of the interface, inside the diffusion sublayer, the molecular diffusion predominates over the turbulence mechanism for the heat transfer. Thus, the film thickness δ is equivalent to the thickness of the diffusion sublayer and is related to the laminar viscous sublayer, δ_o as:

$$\delta=(\alpha/\nu)^{1/n}\delta_o=\delta_o/(\text{Pr})^{1/n} \quad (6)$$

where ν is the kinematic viscosity, α the thermal diffusivity, and n is a constant to be determined experimentally. According to the experimental data for liquid-solid interface, $n=3$ (Azbel, 1981). The thickness of laminar viscous sublayer can be estimated as:

$$\delta_o=5L/[(\phi/2)^{1/2}Re] \quad (7)$$

The value of friction factor ϕ can be calculated by the expression for the drag force on a flat plate wetted on both sides as given by Bird et al. (1960). Thus, the thickness of laminar viscous sublayer δ_o can be estimated by:

$$\delta_o=6.14L/Re^{3/4} \quad (8)$$

where $Re=LU_b/\nu$. Knowing δ and t_c, the bubble-wake-induced enhanced heat transfer h'_{av} can be obtained by Eq. 5.

According to the proposed mechanism, the contact time t_c and the film thickness δ would differ during the passage of each bubble under the condition of periodic bubble injection (chain bubbling) as the bubble rise velocity would differ due to significant bubble-wake interactions. It is noteworthy that the local time-averaged heat-transfer coefficient measured in a freely-bubbling bed is comparable to the local maximum for single-bubble injection in both liquid and liquid-solid systems (Figures 3 and 4). Since Kumar et al. (1992) showed that the

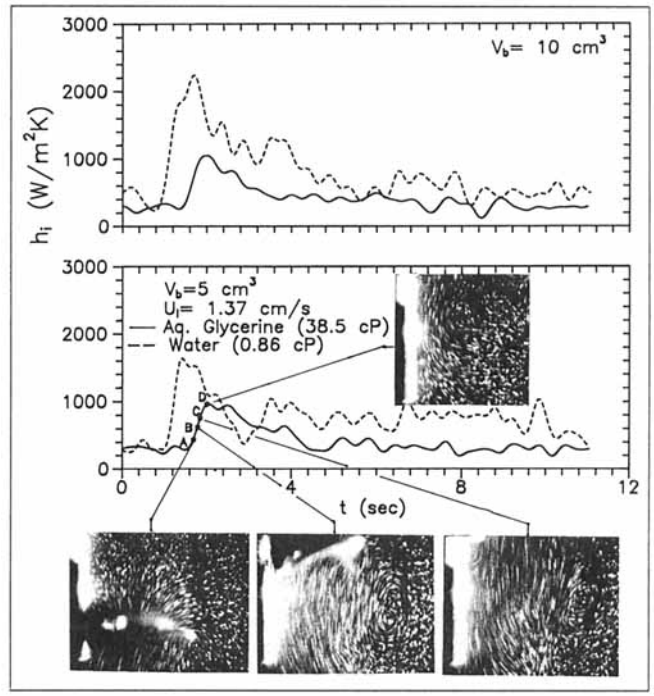

Figure 3. Effects of viscosity and bubble size on instantaneous heat-transfer coefficient due to the passage of bubble in liquids.

characteristic fluid element velocity during the bubble-wake-induced heat-transfer enhancement is equivalent to the absolute bubble rise velocity, it is reasonable to assume that at high bubble injection frequency, the velocity of fluid element near the probe surface over the entire sampling time of 11.2 s is equal to the average in-line bubble rise velocity. Therefore, the contact time for a freely-bubbling bed and a bed with chain bubbling at high bubble injection frequency is given as:

$$t_c=L/U'_{b,av} \quad (9)$$

where $U'_{b,av}$ is the average in-line bubble rise velocity. By following each bubble frame by frame in the video recording over

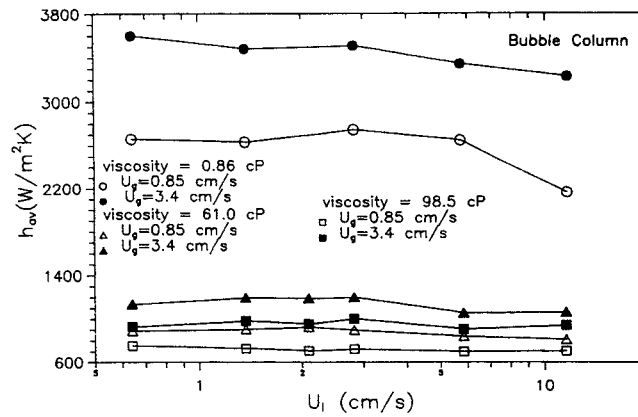

Figure 4. Variations of time-averaged heat-transfer coefficients with gas and liquid velocities in bubble columns with viscous liquids.

a certain distance, the absolute bubble rise velocity of each bubble can be computed from visual signals. The average in-line bubble rise velocity can be obtained by averaging the individual velocities. Alternatively, the bubble interaction/acceleration effect in a stream of bubbles could be taken into account by incorporating an additional wake velocity term in the terminal rise velocity of an isolated bubble. Marks (1973) and Miyahara et al. (1984) regarded wake velocity as the net velocity of the liquid flow near the central axis of the wake and found it to be proportional to the centerline velocity in a batch liquid. Based on the classical wake theory of Schlichting (1979), Miyahara et al. (1991) proposed an empirical equation to predict the actual rise velocity of a bubble in a stream of bubbles as:

$$(U'_{b,\mathrm{av}}/U_b)^{2/3}[(U'_{b,\mathrm{av}}/U_b)-1]=K[g/(U_b f)]^{1/3}(d_e f/U_b) \quad (10)$$

where K is a proportionality constant to be evaluated from the experimental data. The value of K attributes to the magnitude of acceleration effect due to bubble-wake interaction. Miyahara et al. (1991) observed a smaller value of K in gas-liquid-solid fluidized bed compared to that in gas-stagnant liquid systems and concluded that the acceleration effect due to bubble wake is weaker in three-phase systems than that in gas-liquid systems. For chain bubbling in quiescent viscous liquids, Miyahara et al. (1984) proposed the value of $K=2.25$ (for $2.25\times10^{-7}<M<10$). Thus, Eq. 10 along with $K=2.25$ can be used for prediction of average in-line bubble rise velocity in a stream of bubbles. The terminal rise velocity of a single spherical cap bubble can be obtained by using the Davies-Taylor equation (Clift et al., 1978) with the correction for the wall-effect as suggested by Uno and Kintner (1956). Thus,

$$U_b/U_{b,\infty}=[(1/m)(1-d_e/d_c)]^{0.765} \text{ for } d_e/d_c\geq 0.1 \quad (11)$$

where for spherical cap bubbles $U_{b,\infty}=(gd_e/2)^{1/2}$; $m=0.89$ for aqueous glycerin and $m=0.88$ for water. The absolute terminal rise velocity of a single bubble is also measured from visual signals and is found to be in excellent agreement with Eq. 11. The average in-line bubble rise velocity, $U'_{b,\mathrm{av}}$, obtained using Eqs. 10 and 11 are within 10% with those directly measured from visual signals.

Typically for gas-liquid or gas-liquid-solid systems with viscous liquids and large bubbles, $\alpha\approx1\times10^{-7}$ m^2/s, $U'_{b,\mathrm{av}}\approx40$ cm/s, and therefore $t_c=0.064$ s. Using Eqs. 6, 8, and 9, we obtain $\delta\approx0.45\times10^{-3}$ m and $(\alpha t_c)^{1/2}/\delta\approx0.178$. For values of $(\alpha t_c)^{1/2}/\delta<0.30$, typically encountered in bubble columns and three-phase fluidized beds, the relationship between $h'_{\mathrm{av}}\delta/k$ and $(\alpha t_c)^{1/2}/\delta$ can be approximated as linear and inversely proportional. Therefore, Eq. 5 yields:

$$h'_{\mathrm{av}}=C(\rho_l C_{pl}k/t_c)^{1/2} \quad (12)$$

which is the surface renewal/penetration model (shown in Eq. 4) with a different constant C. As mentioned earlier, Tuot and Clift (1973) also reported that the transient heat transfer behind bubbles in a gas-solid fluidized bed can be predicted by the surface renewal/penetration model with a different constant. Thus, the local time-averaged heat transfer behind bubbles in viscous bubble columns can be predicted by an equation of the form:

$$h'_{\mathrm{av}}=C_1(1/t_c)^{1/2} \quad (13)$$

where C_1 depends on liquid properties and is specific for a system. Similarly, the local time-averaged heat-transfer coefficients in gas-liquid-solid systems would be given as:

$$h'_{\mathrm{av}}=C_2(1/t_c)^{1/2} \quad (14)$$

where C_2 is a constant characterizing the specific liquid-solid systems. Constants C_1 and C_2 can be evaluated experimentally for each system and the values of t_c can be obtained from Eq. 9 once the average in-line bubble rise velocity is known. Thus, Eqs. 13 and 14 exhibit that the local heat transfer due to the passage of bubbles increases with the bubble rise velocity. Since, the bubble rise velocity increases with the bed voidage, the enhancement in local heat transfer due to bubble passage also increases with the bed voidage. Furthermore, the equations represent that the heat-transfer due to bubble columns and three-phase fluidized beds is caused by the increased bubble rise velocity due to the increased bubble interactions.

Results and Discussion

Single bubble

Typical heat-transfer signals for a single bubble passage in liquids of different viscosities are shown in Figure 3. In all these signals, as the bubble approaches the probe, the instantaneous local heat-transfer coefficient increases rapidly, attains a maximum value, and then gradually recovers to the initial value. The recovery is quicker in the higher-viscosity liquid due to smaller secondary wake. The flow structure near the probe surface for points A, B, C, and D in the heat-transfer signal is also shown in Figure 3: The vortex structure in viscous liquid ($Re_b=300$) is alternate shedding in contrast to the parallel-shedding vortex structure reported by Kumar et al. (1992) in a low-viscosity liquid ($Re_b=9{,}000$). Nevertheless, bubble wake is still the primary cause for heat-transfer enhancement in viscous systems, and the maximum in the heat-transfer signals lies in the region of high shear flows in the cross flow between primary wake and shedded vortex.

Figure 3 also shows that the maximum in the heat-transfer signal increases with the bubble size, the increase being more pronounced for the lower-viscosity liquid. With increasing bubble size, the strength of circulation in the bubble wake increases due to the increase in the rise velocity of the bubble. However, with increasing viscosity, the heat-transfer enhancement due to single bubble passage decreases due to the rapid decay in the circulation strength of the bubble wake caused by the increased viscous dissipation of vorticity. Also, the size of primary wake decreases with increasing ν, thereby lowering the bubble-wake-induced heat transfer. Crabtree and Bridgwater (1969) reported that in highly viscous liquids ($\nu=8.34$ cm^2/s), no vortex formation is observed, and as ν is reduced a weak systematic vortex pattern is observed which becomes stronger and larger by further reduction of viscosity. After the passage of a bubble, the shed vortices increase in radius and decay in strength at a rate dependent on the kinematic viscosity of the liquid. They further reported that, with liquids of low viscosity, the decay time is longer and the radial growth greater with separate vortices ultimately merging in the experiments

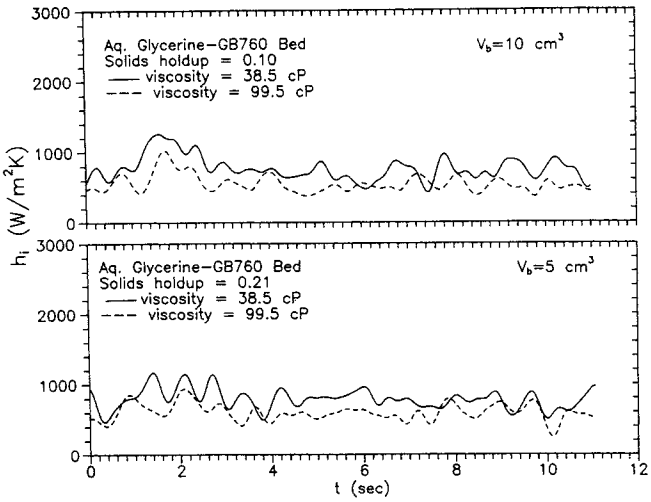

Figure 5. Effects of viscosity and bubble size on instantaneous heat-transfer coefficient due to the passage of bubble in liquid-solid fluidized beds.

with the liquid to form an apparently homogeneous wake (the secondary wake).

Typical heat-transfer signal due to the passage of a bubble in a liquid-solid fluidized bed of 760-μm glass beads (GB760) with varying liquid phase viscosity is shown in Figure 5. The heat-transfer signal is qualitatively similar to the one obtained in liquid systems. However, the local maximum in the signal is diffused and lower compared to that in liquid systems due to the presence of solids causing a reduction in the strength of wake by attenuating the ordered motion or circulation. The local maximum heat transfer is higher in the bed of lower viscosity liquid as observed earlier for liquid systems (Figure 3). Furthermore, the effect of solids holdup on the magnitude of heat-transfer maximum is small in the liquid-solid bed with high-viscosity liquids. A comparison of the relative magnitude of bubble/bubble-wake-induced heat-transfer enhancement in liquid and liquid-solid systems can be obtained by averaging the local instantaneous heat-transfer coefficient h_i over the period of increased heat transfer as:

$$h'_{av} = \frac{1}{(t_f - t_i)} \int_{t_i}^{t_f} h_i dt \qquad (15)$$

where t_i corresponds to the time where the heat transfer starts increasing due to the oncoming bubble and t_f corresponds to the time in the decreasing part of the signal after the maximum behind bubbles where h_i is within 10% of the baseline value.

Chain bubbling

Figures 6 and 7 show the heat-transfer signal due to cyclic/periodic injection of bubbles of initially equal size and spacing in liquid and liquid-solid systems, respectively. For reference, the heat-transfer signals in both systems due to single bubble injection and in freely-bubbling beds (bubble column or three-phase fluidized bed) are also shown in Figures 6 and 7. The solid line is for spherical cap bubbles with a bubble width of 3.69 cm, and the dotted line represents the signal for large slug

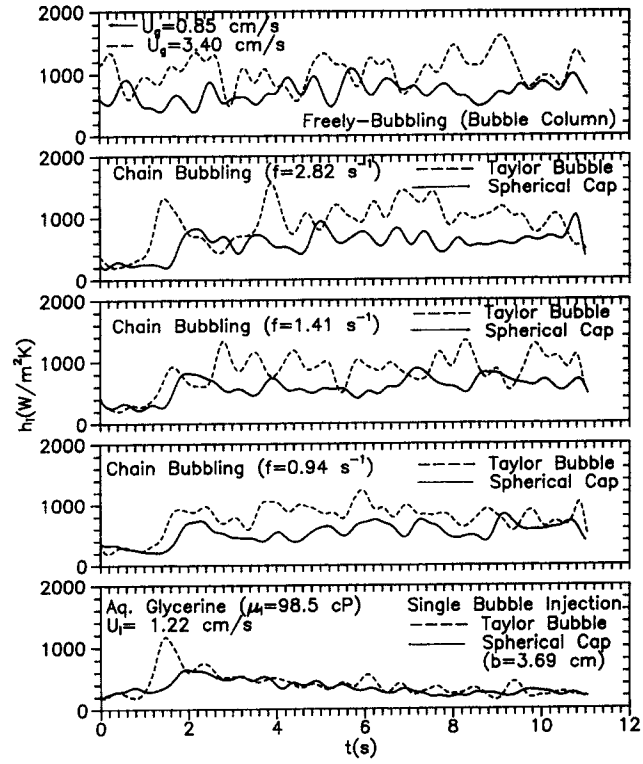

Figure 6. Effects of bubble formation frequency and bubble size on instantaneous heat-transfer coefficient due to chain-bubbling in a highly viscous liquid.

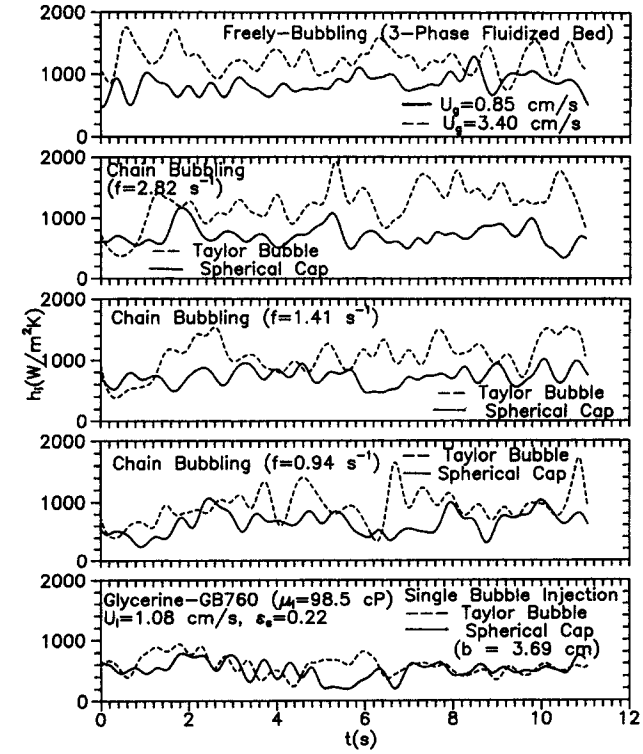

Figure 7. Effects of bubble formation frequency and bubble size on instantaneous heat-transfer coefficient due to chain-bubbling in a liquid-solid fluidized bed with a high viscosity liquid.

or Taylor bubbles. It is evident that the local heat-transfer maximum is higher for chain bubbling than single bubble injection in both liquid and liquid-solid systems. Due to significant bubble-wake interactions or acceleration of the trailing bubble in the wake of the leading one, the renewal at the heat-transfer surface is increased, and the film thickness at the probe surface may be reduced by high shear flow effects. Fan (1989) attributed the acceleration of the trailing bubble to the suction caused by a low-pressure region in the wake immediately below the leading bubble. Miyahara et al. (1991) noted that the acceleration of the trailing bubble is a necessary step for bubble coalescence and reported that the vertical entrainment of the trailing bubble into the near-wake region of the leading bubble is due to the low pressure created in that region, and further acceleration in the very near wake can also be induced by an upward (relative to the bubble) flow along the wake central axis. Several researchers (Komasawa et al., 1980; Miyahara et al., 1991) reported that the extent of interaction between bubbles with unsteady wakes is predominantly affected by the magnitude of the vertical distance between interacting bubbles. In this study, the vertical distance between interacting bubbles can be manipulated by varying the frequency of electric pulse signal or bubble formation frequency, thereby, enabling us to understand the effects of bubble-interaction on the local heat-transfer properties of the bed.

In all the signals (Figures 6 and 7), the bubble injection started at $t = 0$ s, and the local heat transfer gradually increases with time showing local maximum at regular time intervals. The bubble injection/formation frequency, f, is calculated from the number of bubbles injected over the sampling time and verified by counting the number of bubbles passing through the horizontal cross section of the column at the probe location. With the high-viscosity liquid ($\mu_l = 98.5$ cp), the bubble breakup is almost negligible as the higher viscosity is more favorable to coalescence than to breakup. In viscous liquids, the wake structure is stabler than less viscous liquids, and thus there is ample time that two bubbles are brought close enough such that the liquid film separating them is ruptured leading to their coalescence (Otake et al., 1977). While in less viscous liquid, due to unsteady wake structure and shedding of vortex, the probability of coalescence is lowered as the bubbles approach each other. Ostergaard (1966) also observed higher rate of coalescence in viscous liquids and reported that in a liquid of low viscosity, where an approaching bubble may be repelled by the irregular oscillating structure with the result that no coalescence takes place. Miyahara et al. (1991) reported that when the bubble spacing is below a certain distance usually termed as "critical distance" (x_c), the leading bubble starts exerting a noticeable influence on the trailing one, and the trailing bubble can accelerate appreciably toward the leading one and would eventually collide. Otake et al. (1977) reported that the critical distance seems to correspond to the wake length of the leading one. In Figures 6 and 7, at lower bubbling frequency ($f = 0.94$ s^{-1}), the peaks in the heat-transfer signal behind each bubble can be clearly identified. However, as f increases, the individual peaks become undistinguishable at large bubbling frequency ($f = 2.82$ s^{-1}), and the heat-transfer signal with periodic bubble injection starts resembling the freely-bubbling bed. Heat-transfer peaks due to each bubble can be identified when the bubble formation frequency is such that the distance between the successive bubbles at probe location is greater than the critical distance. An idea of the relative magnitude of the enhanced heat transfer by periodic bubble injection can be obtained by averaging h_i with respect to time from the first maximum to the last maximum in the signal, thus ensuring that the effect is only due to the bubbling frequency f which signifies bubble-wake interactions.

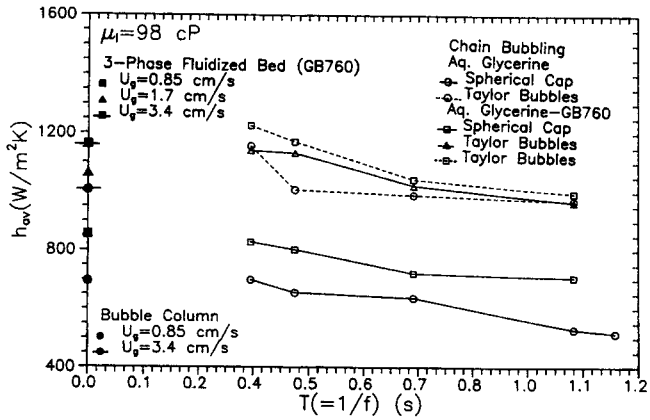

Figure 8. Variations of local time-averaged heat-transfer coefficients with the bubbling frequency in gas-liquid and gas-liquid-solid systems with highly viscous liquids.

Figure 8 shows variations in time-averaged heat-transfer coefficient with the period of injection T ($= 1/f$) under different chain-bubbling conditions. The values at $T = 0$ represent the time-averaged heat-transfer coefficients in freely-bubbling beds: bubble columns and three-phase fluidized beds. The heat transfer by periodic bubble injection is enhanced due to increased bubble-wake interactions as increasing f increases the bubble-wake interactions. At all bubbling frequencies, the heat transfer is found to be higher for the periodic injection of Taylor bubbles than that in the system with the periodic injection of spherical cap bubbles. This is in accordance with the results for single bubble injection signifying that the stronger bubble wake behind Taylor bubbles induces enhanced local mixing than that of spherical cap bubbles. Also, the bubble-wake interactions would be more predominant for Taylor bubbles due to increased critical distance as x_c/d_e is usually a constant. As noted from Figure 8, the increase in time-averaged heat-transfer coefficient with f is higher for bubble injection in liquid systems than that in liquid-solid systems. This is a result of weaker acceleration effects due to bubble wake in liquid-solid systems. Due to the presence of particles, the pressure gradient behind the leading bubble is dampened as a result of particles attenuating the circulation, thereby shortening the critical distance within which the bubbles interact. It is expected that with larger particles, the variation in heat-transfer coefficient with f would become even less significant than that in liquid systems. Similar results are reported for single bubble injection, which showed that the local maximum in heat transfer with respect to the baseline value is more pronounced in liquid systems than that in liquid-solid systems. For large dense particles, the magnitude of local maximum with respect to the baseline value would be relatively small compared to that for the light particles although the baseline values would be higher for heavier particles. This signifies that for three-phase fluidized beds with heavy particles, the bubble-wake effects on

heat transfer are less important than the effects of turbulence caused by solids movement as the average bubble size would be small due to significant bubble breakage caused by particles. However, the bubble-breakage effect is reduced at higher viscosity and due to relatively large size bubbles in viscous systems, the bubble-wake dynamics would predominantly govern the heat-transfer behavior of viscous bubble columns and three-phase fluidized beds. It can be noted from Figure 8 that at high bubbling frequency, the magnitude of local time-averaged heat-transfer coefficients in the simplified liquid and liquid-solid system with periodic/chain bubbling is equal to the heat-transfer coefficients in bubble columns and three-phase fluidized beds under free-bubbling conditions. It is of significant practical importance to note that the increase in the gas velocity with bubbling frequency is not significant, and the average gas flow rate under periodic bubbling conditions is much smaller than that in freely-bubbling beds. Due to smaller size with a size distribution and rise velocities of bubbles in the freely-bubbling bed, the local time-averaged heat transfer in bubble columns and three-phase fluidized beds is equivalent to that under chain bubbling conditions only at a higher gas flow rate ($U_g = 0.85$ cm/s for the coalesced regime and $U_g = 3.4$ cm/s for the slugging regime). Thus, the local heat-transfer coefficients in the simplified system of liquid and liquid-solid bed with single bubble and chain bubble injections are representative of the local heat-transfer properties in freely-bubbling beds (bubble columns and three-phase fluidized beds). In this study, it is observed that the local heat-transfer coefficients at $f = 2.82$ s^{-1} for chain bubbling of spherical cap and Taylor bubbles are equivalent to the heat-transfer values obtained in freely-bubbling beds with coalesced flow ($U_g = 0.85$ cm/s) and slug flow ($U_g = 3.4$ cm/s), respectively.

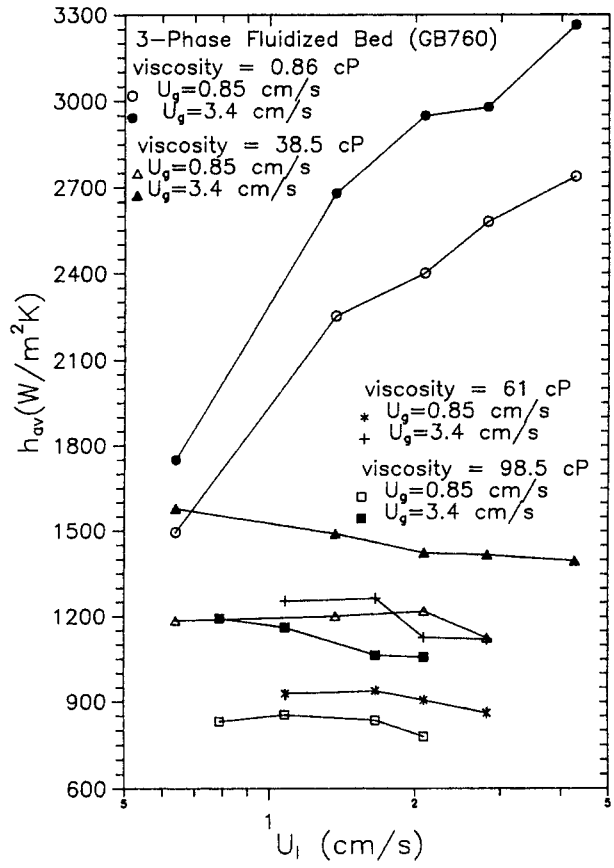

Figure 9. Variations of time-averaged heat-transfer coefficients with gas and liquid velocities in three-phase fluidized beds with viscous liquids.

Freely-bubbling beds

Typical variation of the time-averaged local heat-transfer coefficient with gas and liquid velocities in a bubble column with varying liquid-phase viscosity is shown in Figure 4. The heat-transfer coefficient is almost invariant with U_l, except at higher U_l, where it decreases slightly; the decrease being more pronounced for the bubble column with the low-viscosity liquid. The invariant nature of the heat-transfer coefficients with U_l can be explained based on the vortical strength of the bubble wake. Increasing U_l does not greatly alter the bubble size except at high U_l, thus, the bubble-wake influence on the local heat transfer remains unaltered with changes in U_l resulting in the invariant behavior. In the low-viscosity system, however, at higher liquid velocities ($U_l > 6$ cm/s), the flow conditions change from coalesced to dispersed caused by the shearing and breakage of bubbles which results in lowered heat transfer as the bubble-wake effects are reduced under dispersed flow conditions. The shearing and breakage of bubbles at high U_l are minimal in viscous liquids, and thus the decrease in heat-transfer coefficients is insignificant at high U_l. However, heat transfer in the high-viscosity system with slug flow conditions slightly decreases at higher U_l, since at high U_l, U_g at which slugging of large bubbles is initiated, becomes larger with U_l. Heat transfer in the bubble column significantly increases with the gas velocity at all viscosities primarily due to changes in flow regime resulting in a larger average bubble size. Increased bubble size results in a greater turbulence induced by the bubble wake which enhances the local heat transfer. The flow regime at the low viscosity ($\mu_l = 0.86$ cp) is the coalesced bubble flow, while at higher viscosities ($\mu_l = 61$ cp and 98.5 cp), the coalesced large bubble flow prevails at $U_g = 0.85$ cm/s and the slug flow regime exists at $U_g = 3.4$ cm/s. The local heat transfer is found to be higher in the slug flow regime than that in the coalesced flow regime in viscous bubble columns. This is consistent with the results obtained for single and chain bubble injection in viscous liquid systems as reported earlier.

Figure 9 shows the local heat-transfer behavior in a three-phase fluidized bed with liquids of different viscosities. The flow regime in the three-phase bed with low-viscosity liquid ($\mu_l = 0.86$ cp) is the coalesced bubble flow, while in the bed with high-viscosity liquids ($\mu_l = 38.5$, 61, and 98.5 cp), the coalesced large-bubble flow prevails at $U_g = 0.85$ cm/s, and the slug flow regime is noticed at $U_g = 3.4$ cm/s. In three-phase fluidized beds with highly viscous liquids, a sluggish fluidization with jumping action of the solids is visually observed at high U_g similar to the observation of Patwari et al. (1986). The local heat-transfer coefficient in three-phase fluidization systems with high-viscosity liquids increases with U_g but is relatively independent of U_l. The slight decrease in heat transfer at high U_l in the slug flow regime is due to slightly reduced average bubble size, since at higher U_l, U_g must be increased to maintain the same flow regime. However, in the bed with low-viscosity liquid, heat transfer significantly increases with both gas and liquid velocities. The invariant behavior of heat transfer with U_l in the high-viscosity bed is due to the reduced

mobility and terminal velocity of particles, thereby, having little effects on the heat-transfer behavior. This behavior is similar to that in a bubble column, as in the bed with highly viscous liquids due to significantly reduced particle terminal velocity and larger bubble sizes, the bed can entirely be suspended by the bubble flow without the liquid flow. This indicates that the vortical strength of the bubble wake is unaffected at higher bed porosities in beds with high-viscosity liquids as the effect of particles on attenuating bubble-wake-induced turbulence is significantly small and is relatively independent of the bed expansion. This is in sharp contrast to the low-viscosity three-phase system ($\mu_l = 0.86$ cp) where increasing liquid velocity or bed porosity reduces the concentration of particles, and hence the particle effects on attenuating the circulation in the bubble wake are lowered, thereby significantly enhancing the vortical strength of bubble wake. Hence, in the low-viscosity three-phase bed, heat transfer increases with U_l and ultimately approaches the value in a bubble column.

Figure 10 shows the effects of particle size on the heat-transfer performance of the bed with a highly viscous liquid ($\mu_l = 98.5$ cp). In the three-phase fluidized bed, the particle size effects in the experimental range studied are small at all gas velocities. This is in accordance with the fact that the particle inertia effect on vortical strength of wake is reduced in the high-viscosity liquid due to the reduced terminal velocity and mobility of the particles. For comparison, heat-transfer coefficients in liquid-solid fluidized beds ($\mu_l = 98.5$ cp) of GB760 and GB1000 are also shown in Figure 10. The heat-transfer coefficient in liquid-solid fluidized beds (no gas flow) is measured by the probe located at the center of column in a similar fashion as mentioned previously for three-phase fluidized beds. The magnitude of enhancement in heat transfer in the bubbling system (three-phase fluidized bed) over the nonbubbling system (liquid-solid fluidized bed) is higher for smaller size particles, indicating that the U_t of GB760 is smaller than GB1000, thereby having less effects on the bubble-wake induced heat transfer enhancement which is the primary mechanism for heat transfer in three-phase fluidized beds with small/light particles.

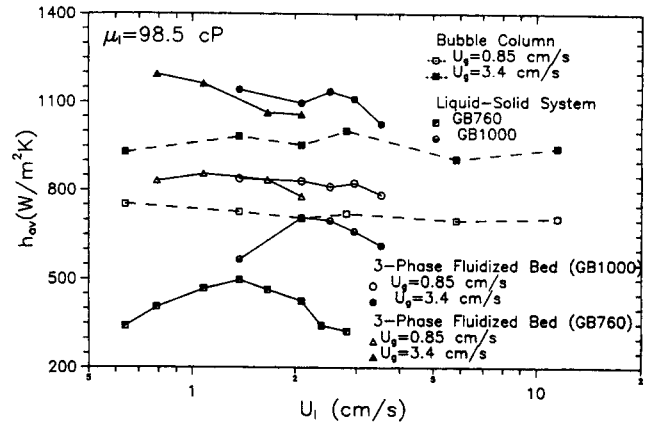

Figure 10. Effects of particle size and liquid velocities at a certain liquid viscosity in bubble columns, liquid-solid fluidized beds, and three-phase fluidized beds.

Comparsion with the model

To validate the model, results obtained theoretically using the proposed model are compared in Table 1 with the experimental results for local time-averaged heat transfer due to bubble with single bubble injection and chain bubbling in viscous liquids. In addition, predicted bubble rise velocity is compared with experimental values. Model-predicted results agree well with experimental results.

To validate the model in freely-bubbling beds, it is necessary to estimate the average bubble rise velocity under such conditions. In freely-bubbling beds (bubble columns and three-phase fluidized beds), Kim et al. (1977) reported that the bubble size and the bubble rise velocity increase with the gas velocity but are relatively insensitive to the liquid velocity. Also, the bubble rise velocity in freely-bubbling beds is essentially a function only of the bubble size similar in nature to Davies-Taylor bubbles. Based on their experiments with various liquids, Kim et al. (1977) proposed correlations for the bubble rise velocity and noted that in gas-liquid systems:

$$U'_{b,\mathrm{av}} \propto U_g^{0.341} \tag{16}$$

whereas in gas-liquid-solid systems:

$$U'_{b,\mathrm{av}} \propto U_g^{0.339} \tag{17}$$

Bhavaraju et al. (1978) also reported that at moderately high gas rates in bubble columns with viscous liquids (30–700 cp), the bubble diameter was found to increase at a rate proportional to one-third power of gas rate; since the frequency of

Table 1. Model-Predicted Heat-Transfer Enhancement Due to Bubbles vs. Experimental Results

Cases	μ_l (cp)	U_b, $U'_{b,\mathrm{av}}$ (cm/s) Exp.	U_b, $U'_{b,\mathrm{av}}$(cm/s) Model	δ (mm)	h'_{av} (W/m^2·K) Exp.	h'_{av} (W/m^2·K) Model
Single bubble, $b = 3.42$ cm	38.5	27.8	27.85	0.414	684.10	663.90
Single bubble, $b = 4.3$ cm	38.5	28.8	28.83	0.403	693.87	680.46
Single bubble, $b = 3.69$ cm	98.5	28.06	28.20	0.587	492.25	467.94
Chain bubbling, $b = 3.69$ cm $f = 0.94$ s^{-1}	98.5	36.23	40.1	0.487	627.98	560.68
Chain bubbling, $b = 3.69$ cm $f = 2.82$ s^{-1}	98.5	44.22	50.4	0.419	698.10	646.973

bubble formation remains constant, the relationship between the bubble rise velocity and the gas flow rate is of the form $U'_{b,av} \propto U_g^{0.333}$ similar to Eq. 16. Thus, for bubble-columns using Eqs. 13 and 16, the dependency of h_{av} on U_g is of the form:

$$h_{av} \propto U_g^{0.172} \tag{18}$$

Comparing the experimental values of h_{av} obtained in this study for different U_g at same U_l (Figure 4), it is found that Eq. 18 holds well. It is remarkable to note that a relationship of the form shown in Eq. 18 obtained primarily from a mechanistic viewpoint has also been reported by several researchers based on their correlation of experimental data. For example, Nishikawa et al. (1977) obtained a relationship of the form $h_{av} \propto U_g^{0.161}$ in the bubble column based on his experimental data for viscous liquids under moderate gas velocities. For three-phase fluidized beds, using Eqs. 14 and 17:

$$h_{av} \propto U_g^{0.170} \tag{19}$$

Comparing with experimental results obtained in this study (Figure 9), Eq. 19 holds well. Thus, the increased heat transfer in freely-bubbling beds is mainly due to increased bubble rise velocity caused by the increased bubble-wake interactions and is primarily a function of the superficial gas velocity. From the local heat-transfer performance point of view, the difference between a freely-bubbling bed and a simplified system with single bubble injections is mainly due to significantly higher bubble rise velocities, resulting in an enhanced heat-transfer renewal and reduced film thickness at the probe surface due to high shear flows causing a much higher local heat transfer. Thus, Eqs. 13 and 14 may be used to describe the heat-transfer characteristics of viscous bubble columns and three-phase fluidized beds, respectively.

Conclusions

Local heat-transfer studies are performed with viscous Newtonian liquids in freely-bubbling beds (bubble columns and three-phase fluidized beds) and in liquid and liquid-solid systems by introducing a single bubble or a chain of bubbles. A peak in the local heat-transfer signal is observed due to the bubble passage in liquid and liquid-solid systems, and the peak is observed to lie in the high shear flow region in the wake. The magnitude of the local heat-transfer maximum behind bubbles is reduced as the liquid viscosity increases due to the lesser circulation strength in the bubble wake as a result of increased viscous dissipation of vorticity. The local maximum heat-transfer coefficients behind a single bubble in liquid and liquid-solid systems with viscous liquids are comparable to the local time-averaged heat-transfer coefficients in freely-bubbling beds, thereby signifying that the bubble-wake-induced heat-transfer enhancement is the primary mechanism of heat transfer in bubble columns and three-phase fluidized beds with viscous liquids.

Local maxima in the heat-transfer coefficient behind bubbles in the case of cyclic/periodic injection of bubbles are higher than those in a single bubble due to bubble-wake interactions. Because of the rapid acceleration of bubbles and increased average bubble rise velocity, heat transfer is significantly enhanced primarily as a result of increased surface renewal at the probe surface and reduced film thickness caused by shear effects. With an increase in the bubbling frequency, heat transfer is further enhanced, and ultimately at higher frequencies, the heat transfer characteristics under chain bubbling conditions start resembling those in a freely-bubbling bed.

The heat transfer significantly increases with U_g in a freely-bubbling bed due to the increased average bubble size and average bubble rise velocity. Local heat transfer is found to be higher in the slug flow regime than that in the coalesced flow regime in bubble columns and three-phase fluidized beds with viscous liquids. Similar to bubble columns, the local heat transfer in three-phase fluidized beds with viscous liquids shows an invariant behavior with respect to U_l due to the reduced mobility and terminal velocity of particles. This is in sharp contrast to the three-phase fluidized beds with low-viscosity liquids, where increasing U_l significantly increases heat transfer. Particle size effects on heat transfer are also found to be small in viscous systems.

A mechanistic model is proposed to account for the local heat-transfer behavior in the bed due to the passage of bubbles in liquid and liquid-solid systems with high viscous liquids. The heat-transfer enhancement due to the bubble under single and chain bubble injections is well predicted by the model. The model is extended to freely-bubbling beds (bubble columns and three-phase fluidized beds). The model suggests that for a given system with known physical properties of the liquid and solid phases, the local heat transfer in the bed is solely characterized by the average bubble rise velocity which depends on the gas velocity and the bed expansion. The model holds well for bubble columns and three-phase fluidized beds with viscous liquids and provides a mechanistic understanding of the heat-transfer behavior of the bed.

Acknowledgment

This work was supported by NSF Grant No. INT-9024546.

Notation

b = bubble width, cm
C_{pl} = specific heat capacity of liquid, J/kg·K
d_c = column diameter, cm
d_e = equivalent bubble diameter, cm
d_p = particle diameter, μm
f = bubble injection frequency during chain bubbling, s^{-1}
g = acceleration due to gravity, cm/s^2
h'_{av} (model) = time-averaged heat-transfer coefficient over t_c, $W/m^2 \cdot K$
h'_{av} (expt.) = time-averaged heat-transfer coefficient defined in Eq. 15, $W/m^2 \cdot K$
h_{av} = time-averaged heat-transfer coefficient over the sampling time, $W/m^2 \cdot K$
h_i = instantaneous heat-transfer coefficient, $W/m^2 \cdot K$
k = thermal conductivity, W/m·K
K = empirical constant to account for extent of interaction
L = length of the heat-transfer probe, cm
m = constant in Eq. 11
M = Morton number
Pe = Peclet number
Pr = Prandtl number
Q = time-averaged heat flux, W/m^2
Re = Reynolds number based on probe length
Re_b = Reynolds number based on bubble width
t = real time, s
t_c = contact time, s
t_f = time corresponding to the upper limit for averaging h_i, s

t_i = time corresponding to the lower limit for averaging h_i, s
T = time period of bubble injections
T_{si} = instantaneous probe surface temperature, K
T_∞ = bulk temperature, K
U_b = absolute bubble rise velocity, cm/s
$U_{b\infty}$ = absolute bubble rise velocity in infinite medium, cm/s
$U'_{b,av}$ = average in-line bubble rise velocity, cm/s
U_g = superficial gas velocity, cm/s
U_l = superficial liquid velocity cm/s
U_t = particle terminal velocity, cm/s
V_b = bubble volume, cm^3
x_c = critical interaction distance, cm

Greek letters

α = thermal diffusivity, cm^2/s
δ = average film thickness, mm
δ_o = average thickness of laminar sublayer, mm
ΔT_i = instantaneous temperature difference between probe surface and bulk, K
ϵ_l = bed porosity
μ_l = liquid viscosity, cp
ν = liquid kinematic viscosity, cm^2/s
ρ_l = liquid density, g/cm^3
ϕ = friction factor

Literature Cited

Azbel, D., *Two-Phase Flows in Chemical Engineering*, Cambridge Univ. Press, Cambridge, London (1981).

Bhavaraju, S. M., T. W. F. Russell, and H. W. Blanch, "The Design of Gas Sparged Devices for Viscous Liquid Systems," *AIChE J.*, **24**, 454 (1978).

Bird, R. B., W. E. Stewart, and E. N. Lightfoot, *Transport Phenomena*, p. 203, Wiley, New York (1960).

Clift, R., J. R. Grace, and M. E. Webber, *Bubble Drops and Particles*, Academic Press, New York (1978).

Crabtree, J. R., and J. Bridgwater, "The Wakes Behind Two-Dimensional Air Bubbles," *Chem. Eng. Sci.*, **22**, 1517 (1967).

Deckwer, W.-D., Reaktionstechnik in Blasensäulen, Salle + Saureländer, Frankfurt/Main (D), Germany (1985); English translation available as *Bubble Column Reactors*, Wiley, Chichester, England (1992).

Epstein, N., "Review: Three-Phase Fluidization-Some Knowledge Gaps," *Can. J. Chem. Eng.*, **59**, 649 (1981).

Fan, L.-S., *Gas-Liquid-Solid Fluidization Engineering*, Butterworths, Stoneham, MA (1989).

Fan, L.-S., and K. Tsuchiya, *Bubble Wake Dynamics in Liquids and Liquid-Solid Suspensions*, Butterworth-Heinemann, Stoneham, MA (1990).

Grandjean, B. P. A., I. Nikov, P. J. Carreau, and J. Paris, "Viscosity Effects in Cocurrent Three-Phase Fluidization," *AIChE J.*, **36**, 1613 (1990).

Kang, Y., I. S. Suh, and S. D. Kim, "Heat Transfer Characteristics of Three Phase Fluidized Beds," *Chem. Eng. Commun.*, **34**, 1 (1985).

Kato, Y., K. Uchida, T. Kago, and S. Morooka, "Liquid Holdup and Heat Transfer Coefficient Between Bed and Wall in Liquid-Solid and Gas-Liquid-Solid Fluidized Beds," *Powder Technol.*, **28**, 173 (1981).

Kim, S. D., C. G. J. Baker, and M. A. Bergougnou, "Bubble Characteristics in Three-Phase Fluidized Beds," *Chem. Eng. Sci.*, **32**, 1299 (1977).

Kim, S. D., and A. Laurent, "The State of Knowledge on Heat Transfer in Three-Phase Fluidized Beds," *Int. Chem. Eng.*, **31**, 284 (1991).

Komasawa, I., T. Otake, and M. Kamojima, "Wake Behavior and its Effect on Interaction Between Spherical Cap Bubbles," *J. Chem. Eng. Japan*, **13**, 103 (1980).

Kumar, S., K. Kusakabe, K. Raghunathan, and L.-S. Fan, "Mechanism of Heat Transfer in Bubbly Liquid and Liquid-Solid Systems: Single Bubble Injection," *AIChE J.*, **38**, 733 (1992).

Marks, C. H., "Measurements of the Terminal Velocity of Bubbles Rising in a Chain," *Trans. ASME, J. Fluid Eng.*, **95**, 17 (1973).

Miyahara, T., S. Kaseno, and T. Takahashi, "Studies on Chains of Bubbles Rising Through Quiescent Liquid," *Can. J. Chem. Eng.*, **62**, 186 (1984).

Miyahara, T., K. Tsuchiya, and L.-S. Fan, "Effect of Turbulent Wake on Bubble-Bubble Interaction in a Gas-Liquid-Solid Fluidized Bed," *Chem. Eng. Sci.*, **46**, 2368 (1991).

Nishikawa M., H. Kato, and K. Hashimoto, "Heat Transfer in Aerated Tower Filled with Non-Newtonian Liquid," *Ind. Eng. Chem. Process Des. Dev.*, **16**, 133 (1977).

Ostergaard, K., "On the Growth Of Air Bubbles Formed at a Single Orifice in a Water Fluidized Bed," *Chem. Eng. Sci.*, **21**, 470 (1966).

Otake, T., S. Tone, K. Nakao, and Y. Mitsuhashi, "Coalescence and Breakup of Bubbles in Liquids," *Chem. Eng. Sci.*, **32**, 377 (1977).

Patwari, A. N., K. Nguyen-Tien, A. Schumpe, and W.-D. Deckwer, "Three-Phase Fluidized Beds with Viscous Liquid: Hydrodynamics and Mass Transfer," *Chem. Eng. Commun.*, **40**, 49 (1986).

Schlichting, H., *Boundary Layer Theory*, 7th ed., McGraw-Hill, New York (1979).

Toor, H. L., and J. M. Marchello, "Film-Penetration Model for Mass and Heat Transfer," *AIChE J.*, **4**, 97 (1958).

Tuot, J., and R. Clift, "Heat Transfer Around Single Bubbles in a Two-Dimensional Fluidized Bed," *AIChE Symp. Ser.*, **69**, 78 (1973).

Uno, S., and R. C. Kintner, "Effect of Wall Proximity on the Rate of Rise of Single Air Bubbles in a Quiescent Liquid," *AIChE J.*, **2**, 420 (1956).

Wasan, D. T., and M. S. Ahluwalia, "Consecutive Film and Surface Renewal Mechanism for Heat or Mass Transfer from a Wall," *Chem. Eng. Sci.*, **24**, 1535 (1969).

Zaidi, A., W. D. Deckwer, A. Mrani, and B. Benchekchou, "Hydrodynamics and Heat Transfer in Three-Phase Fluidized Beds with Highly Pseudoplastic Solutions," *Chem. Eng. Sci.*, **45**, 2235 (1990).

Manuscript received Apr. 26, 1993, and revision received Aug. 23, 1993.